

# BUCKLING OF LAMINATED COMPOSITE SPHERICAL SHELL CAP

K.S. Sai Ram\*

## Abstract

*The buckling of laminated composite spherical shell cap with and without a cutout subjected to transverse load is investigated. The geometrical non-linear analysis is carried out using the finite element method based on the first-order shear deformation theory. An eight noded degenerated isoparametric shell element with five degrees of freedom at each node is considered. The geometric non-linear behaviour and the collapse pressures with the associated mode shapes are presented for simply supported and clamped symmetrically and anti-symmetrically laminated cross-ply spherical shell cap without a cutout subjected to uniform normal pressure. The dependence of collapse pressure on the size of a central circular cutout is also studied.*

## Nomenclature

a	= radius of the circular base of the spherical shell cap	$P_o$	= intensity of normal pressure
E	= Young's modulus of isotropic material	$P_n$	= $P_o (a/t)^4/E_2$
$E_1, E_2$	= Young's moduli along 1 and 2 axes of a lamina	$P_{nc}$	= normalised collapse pressure
FEM	= Finite Element Method	$Q_x, Q_y$	= transverse shear forces per unit length
$G_{12}, G_{13}, G_{23}$	= shear moduli in 1-2, 1-3 and 2-3 planes of a lamina, respectively	R	= radius of curvature
H	= depth of spherical shell cap	$R_x, R_y$	= Radii of curvature in XZ and YZ planes, respectively
$K_x, K_y, K_{xy}$	= curvatures of a shell	t	= thickness of a shell
$l_1, m_1, n_1$	= direction cosines between x & X, x & Y, x & Z axes, respectively	u, v, w	= displacement components along x, y and z axes, respectively
$l_{1i}, m_{1i}, n_{1i}$	= direction cosines between x & X, x & Y, x & Z axes, respectively at a node i	$u_o, v_o, w_o$	= displacements of the mid-surface along x, y and z axes, respectively
$l_2, m_2, n_2$	= direction cosines between y & X, y & Y, y & Z axes, respectively	$U_{oi}, V_{oi}, W_{oi}$	= displacements of the mid-surface along X, Y and Z axes, respectively at a node i
$l_{2i}, m_{2i}, n_{2i}$	= direction cosines between y & X, y & Y, y & Z axes, respectively at a node i	$u_{o,x}, v_{o,x}, w_{o,x}$ etc.	= derivatives of a variable with respect to a subscript
$M_x, M_y, M_{xy}$	= moment resultants per unit length	W	= central deflection of a panel along Z-axis
$l_3, m_3, n_3$	= direction cosines between z & X, z & Y, z & Z axes, respectively	$W_n$	= W/t
$l_{3i}, m_{3i}, n_{3i}$	= direction cosines between z & X, z & Y, z & Z axes, respectively at a node i	x, y, z	= local Cartesian co-ordinate axes at any point on the mid-surface of a shell, x and y axes being tangential to the mid-surface whereas z-axis is normal the mid-surface
n	= number of layers	X, Y, Z	= global Cartesian co-ordinate axes
$N_i$	= shape function of the finite element at a node i	$X_i, Y_i, Z_i$	= global co-ordinates of a node i
$N_{ix}, N_{iy}$	= derivatives of $N_i$ with respect to x and y axes, respectively	$Z_i$	
$N_x, N_y, N_{xy}$	= membrane forces per unit length	$z_k, z_{k-1}$	= top and bottom distances of a lamina from the mid-surface
		$\alpha$	= shear correction factor
		$\gamma_{xy}$	= shear strain in xy plane at a distance z from the mid-surface

\* Professor, Department of Civil Engineering, RVR & JC College of Engineering, Chowdavaram, Guntur-522 019, India

Email : sairamks@yahoo.com

Manuscript received on 26 Apr 2004; Paper reviewed, revised and accepted on 08 Oct 2004

$\gamma_{xy0}$	= shear strain of the mid-surface in xy plane
$\gamma_{xz}, \gamma_{yz}$	= transverse shear strains at a distance z from the mid-surface
$\epsilon_x, \epsilon_y$	= strains along x and y axes, respectively at a distance z from the mid-surface
$\epsilon_{x0}, \epsilon_{y0}$	= strains of the mid-surface along x and y axes, respectively
$\eta$	= local natural co-ordinate of an element
$\theta$	= fibre orientation in a lamina with reference to x-axis
$\theta_x, \theta_y$	= rotations of a shell about x and y axes, respectively
$\theta_{xi}, \theta_{yi}$	= rotations of a shell about x and y axes, respectively at a node i
$\nu$	= Poisson's ratio of isotropic material
$\nu_{12}, \nu_{21}$	= Poisson's ratios with respect 1 and 2 axes of a lamina
$\xi$	= local natural coordinate of an element
$\sigma_x, \sigma_y$	= normal stresses along x and y axes, respectively
$\tau_{xy}, \tau_{xz}$	= shear stresses in xy, xz and yz planes, respectively
$\tau_{yz}$	= shear stresses in yz planes, respectively
$\phi_x, \phi_y$	= shear rotations in xz and yz planes, respectively

### Introduction

Fibre reinforced plastic laminated composite shells find wide applications in aerospace and other industries due to their advantages like high specific strength, high specific stiffness and light weight properties over conventional metal shells. Since these are very thin, they undergo buckling for axial and transverse loading. Spherical shells are used for many structures such as aerospace vehicles, roof domes, pressure vessels and submarines. Thus, the buckling of laminated composite spherical shell cap is an important engineering problem to be investigated. The presence of a central circular cutout affects the buckling strength of laminated composite spherical shell cap.

The study of buckling of composite cylindrical shell panels subjected to axial compression, using a geometric non-linear analysis, has been considered by many researchers [1-12]. The study of buckling of composite spherical shells using a geometric non-linear analysis has been considered by a few researchers [13-16]. Xu [13] investigated the large deformation behaviour of symmetrically laminated shallow spherical shells using Bessel-Fourier series approach. Narasimhan and Alwar [14]

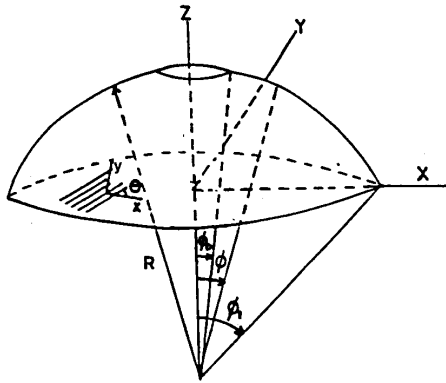
solved the problem of axisymmetric large deformation behaviour of clamped anti-symmetrically laminated spherical shell using Chebyshev-Galerkin spectral method based on deep shell theory. Estimates of snap pressures for symmetrically laminated cross-ply spherical shell caps obtained with deep shell theory were compared with those obtained by Xu [13]. Estimates of snap pressures for anti-symmetrically laminated cross-ply spherical shell caps were also presented. Aleksander Muc [15] investigated the buckling of axisymmetric clamped composite shells of revolution like spherical caps, torispheres and hemi-spheres using linear buckling analysis and non-linear computer program. It was observed that the linear buckling analysis give completely wrong predictions of buckling pressures, types of failure and variations of buckling pressures with fibre orientations. Sai Ram and Sreedhar Babu [16] investigated the buckling response of laminated composite spherical shell panels subjected to transverse load using a higher-order shear deformation theory.

From the above review of literature it is clear that the buckling of simply supported laminated composite spherical shell cap and the buckling of laminated composite spherical shell cap with a cutout has not been considered. Therefore, in this paper the buckling of composite spherical shell cap subjected to external pressure is thoroughly investigated. Geometric non-linear analysis is carried out using the finite element method with an eight noded degenerated isoparametric shell element based on the first-order shear deformation theory. A Lagrangian approach is used for this purpose. The non-linear behaviour and the collapse pressures with the associated mode shapes are presented for simply supported and clamped symmetrically and anti-symmetrically laminated cross-ply spherical shell caps subjected to uniformly distributed normal pressure. The dependence of collapse pressure on the size of a central circular cutout is also studied.

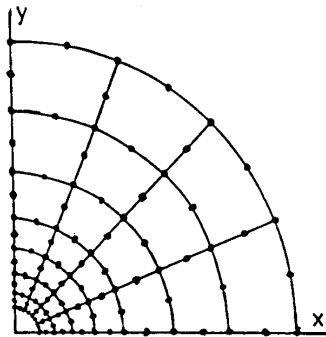
### Governing Equations

Consider a laminated shell of uniform thickness, consisting of a number thin laminae, each of which may be arbitrarily oriented at an angle  $\theta$  with reference to the x-axis of the local coordinate system (Fig.1a). The displacements along the local coordinate axes x, y and z at any point in the shell are assumed as

$$\begin{aligned} u &= u_o + z\theta_y, \\ v &= v_o + z\theta_x, \\ w &= w_o \end{aligned} \quad (1)$$



a) Geometry and fibre orientation



b) Discretisation details for a quarter

Fig. 1 Spherical shell cap with a central circular cut-out

The strains at any point in the shell along the local coordinate axes x, y and z are expressed as

$$\begin{aligned}
 \epsilon_x &= u_{,x} = \epsilon_{xo} + zK_x, \\
 \epsilon_y &= v_{,y} = \epsilon_{yo} + zK_y, \\
 \gamma_{xy} &= u_{,y} + v_{,x} = \gamma_{xyo} + zK_{xy}, \\
 \gamma_{xz} &= u_{,z} + w_{,x} = \phi_x, \\
 \gamma_{yz} &= v_{,z} + w_{,y} = \phi_y,
 \end{aligned} \tag{2}$$

where

$$\begin{aligned}
 \epsilon_{xo} &= u_{o,x} + (w_{o,x})^2/2, \quad \epsilon_{yo} = v_{o,y} + (w_{o,x})^2/2, \\
 \gamma_{xyo} &= u_{o,y} + v_{o,x} + w_{o,x}w_{o,y}, \\
 K_x &= \theta_{y,x}, \quad K_y = -\theta_{x,y}, \quad K_{xy} = \theta_{y,y} - \theta_{x,x}, \\
 \phi_x &= \theta_y + w_{o,x}, \quad \phi_y = -\theta_x + w_{o,y}
 \end{aligned} \tag{3}$$

The incremental strains of the shell along local coordinate axes x, y and z axes are given by

$$\begin{aligned}
 d\epsilon_{xo} &= (du_{o,x} + w_{o,x}(dw_{o,x}), d\epsilon_{yo} = (dv_{o,y} + w_{o,y}(dw_{o,y}), \\
 d\gamma_{xyo} &= (du_{o,y} + (dv_{o,x} + w_{o,x}(dw_{o,y} + w_{o,y}(dw_{o,x}), \\
 dK_x &= (d\theta_{y,x}), dK_y = -(d\theta_{x,y}), dK_{xy} = (d\theta_{y,y} - (d\theta_{x,x}), \\
 d\phi_x &= d\theta_y + (dw_{o,x}), d\phi_y = -d\theta_x + (dw_{o,y}), \tag{4}
 \end{aligned}$$

The stress-strain relations of a lamina with respect to x,y and z axes are given by

$$\begin{bmatrix} \sigma_x \\ \sigma_y \\ \tau_{xy} \end{bmatrix} = \begin{bmatrix} \bar{Q}_{11} & \bar{Q}_{12} & \bar{Q}_{16} \\ \bar{Q}_{12} & \bar{Q}_{22} & \bar{Q}_{26} \\ \bar{Q}_{16} & \bar{Q}_{26} & \bar{Q}_{66} \end{bmatrix} \begin{bmatrix} \epsilon_x \\ \epsilon_y \\ \gamma_{xy} \end{bmatrix}$$

$$\text{or } \{\sigma\} = [\bar{Q}_{ij}]_k \{\epsilon\}, \quad (i,j = 1, 2, 6) \tag{5a}$$

$$\begin{bmatrix} \tau_{xz} \\ \tau_{yz} \end{bmatrix} = \begin{bmatrix} \bar{Q}_{44} & \bar{Q}_{45} \\ \bar{Q}_{45} & \bar{Q}_{55} \end{bmatrix} \begin{bmatrix} \gamma_{xz} \\ \gamma_{yz} \end{bmatrix}$$

$$\text{or } \{\tau\} = [\bar{Q}_{ij}]_k \{\gamma\}, \quad (i,j = 4, 5) \tag{5b}$$

$[\bar{Q}_{ij}]_k$  in equations (5) is defined as

$$[\bar{Q}_{ij}]_k = [T_1]^{-1} [Q_{ij}]_k [T_1]^{-T}, \quad (i, j = 1, 2, 6) \tag{6a}$$

$$[\bar{Q}_{ij}]_k = [T_2]^{-1} [Q_{ij}]_k [T_2], \quad (i, j = 4, 5) \tag{6b}$$

in which

$$[T_1] = \begin{bmatrix} \cos^2\theta & \sin^2\theta & 2\sin\theta \cos\theta \\ \sin^2\theta & \cos^2\theta & -2\sin\theta \cos\theta \\ -\sin\theta \cos\theta & \sin\theta \cos\theta & \cos^2\theta - \sin^2\theta \end{bmatrix},$$

$$[T_2] = \begin{bmatrix} \cos\theta & -\sin\theta \\ \sin\theta & \cos\theta \end{bmatrix},$$

$$[Q_{ij}]_k = \begin{bmatrix} Q_{11} & Q_{12} & 0 \\ Q_{12} & Q_{22} & 0 \\ 0 & 0 & Q_{66} \end{bmatrix}, \quad (i, j = 1, 2, 6)$$

$$[Q_{ij}]_k = \begin{bmatrix} Q_{44} & 0 \\ 0 & Q_{55} \end{bmatrix}, \quad (i, j = 4, 5)$$

in which  $Q_{11} = E_1/(1-\nu_{12}\nu_{21})$ ,  $Q_{12} = \nu_{12}E_2/(1-\nu_{12}\nu_{21})$ ,  
 $Q_{22} = E_2/(1-\nu_{12}\nu_{21})$ ,  $Q_{66} = G_{12}$ ,  $Q_{44} = G_{13}$ ,  $Q_{55} = G_{23}$ .

The various stress resultants are given by

$$\begin{aligned} (N_x, N_y, N_{xy}) &= \sum_{k=1}^n \int_{z_{k-1}}^{z_k} (\sigma_x, \sigma_y, \tau_{xy}) dz, \\ (M_x, M_y, M_{xy}) &= \sum_{k=1}^n \int_{z_{k-1}}^{z_k} (\sigma_x, \sigma_y, \tau_{xy}) z dz, \\ (Q_x, Q_y) &= \sum_{k=1}^n \int_{z_{k-1}}^{z_k} (\tau_{xz}, \tau_{yz}) dz \end{aligned} \quad (7)$$

From equations (2), (5) and (7), the incremental constitutive equations of the shell are obtained as

$$\{dF\} = [D] \{d\chi\}, \quad (8)$$

where

$$\{dF\} = \{dN_x, dN_y, dN_{xy}, dM_x, dM_y, dM_{xy}, dQ_x, dQ_y\}^T,$$

$$\{d\chi\} = \{d\varepsilon_{x0}, d\varepsilon_{y0}, d\gamma_{xy0}, dK_x, dK_y, dK_{xy}, d\phi_x, d\phi_y\}^T.$$

The elasticity matrix in equation (8) may be expressed as

$$[D] = \begin{bmatrix} [A_{ij}] & [B_{ij}] & [0] \\ [B_{ij}] & [D_{ij}] & [0] \\ [0] & [0] & [A_{pq}] \end{bmatrix}$$

in which

$$(A_{ij}, B_{ij}, D_{ij}) = \sum_{k=1}^n \int_{z_{k-1}}^{z_k} [\bar{Q}_{ij}]_k (1, z, z^2) dz, \quad (i, j = 1, 2, 6)$$

$$(A_{pq}) = \alpha \sum_{k=1}^n \int_{z_{k-1}}^{z_k} [\bar{Q}_{ij}]_k dz, \quad (p, q = 4, 5)$$

### Finite Element Formulation

An eight noded degenerated isoparametric shell element [17,18] is considered in the present analysis. Five degrees of freedom are considered at each node. The tangent stiffness matrix and incremental nodal load vector of the element are derived using the principle minimum potential energy. The geometry of the element is defined by the global coordinates X, Y and Z. That is

$$X = \sum_{i=1}^8 N_i X_i, \quad Y = \sum_{i=1}^8 N_i Y_i, \quad \text{and} \quad Z = \sum_{i=1}^8 N_i Z_i$$

The displacements at any point in the element are expressed as

$$\begin{aligned} u_o &= \sum_{i=1}^8 N_i (l_1 U_{oi} + m_1 V_{oi} + n_1 W_{oi}), \\ v_o &= \sum_{i=1}^8 N_i (l_2 U_{oi} + m_2 V_{oi} + n_2 W_{oi}), \\ w_o &= \sum_{i=1}^8 N_i (l_3 U_{oi} + m_3 V_{oi} + n_3 W_{oi}), \\ \theta_x &= \sum_{i=1}^8 N_i (E_{11i} \theta_{xi} + E_{12i} \theta_{yi}), \\ \theta_y &= \sum_{i=1}^8 N_i (E_{21i} \theta_{xi} + E_{22i} \theta_{yi}), \end{aligned} \quad (9)$$

where

$$E_{11i} = l_1 l_{1i} + m_1 m_{1i} + n_1 n_{1i} ,$$

$$E_{12i} = l_1 l_{2i} + m_1 m_{2i} + n_1 n_{2i} ,$$

$$E_{21i} = l_2 l_{1i} + m_2 m_{1i} + n_2 n_{1i} ,$$

$$E_{22i} = l_2 l_{2i} + m_2 m_{2i} + n_2 n_{2i}$$

**Elements Stiffness Matrix**

Substituting equations (9) in equations (4), the incremental strain vector of the element is represented in the form

$$\{d\chi\} = \left[ [B^L] + [B^{NL}] \right] \{d\delta^e\} , \tag{10}$$

where

$$\{d\delta^e\} = \{dU_{o1}, dV_{o1}, dW_{o1}, d\theta_{x1}, d\theta_{y1}, \dots\}$$

$$dU_{o8}, dV_{o8}, dW_{o8}, d\theta_{x8}, d\theta_{y8} \}^T$$

and the non-zero elements of linear and non-linear incremental strain-displacement matrices  $[B^L]$  and  $[B^{NL}]$  are given in Appendix.

The linear stiffness matrix (due to small displacement) of the element is given by

$$[K^{eL}] = \int_{-1}^1 \int_{-1}^1 [B^L]^T [D] [B^L] |J| d\xi d\eta , \tag{11}$$

where  $|J|$  is the determinant of the Jacobian matrix  $[J]$  and is expressed as

$$[J] = \begin{bmatrix} x_{,\xi} & y_{,\xi} \\ x_{,\eta} & y_{,\eta} \end{bmatrix} ,$$

in which

$$x_{,\xi} = l_1 X_{,\xi} + m_1 Y_{,\xi} + n_1 Z_{,\xi} ,$$

$$x_{,\eta} = l_2 X_{,\eta} + m_2 Y_{,\eta} + n_2 Z_{,\eta} ,$$

$$y_{,\xi} = l_1 X_{,\xi} + m_1 Y_{,\xi} + n_1 Z_{,\xi} ,$$

$$y_{,\eta} = l_2 X_{,\eta} + m_2 Y_{,\eta} + n_2 Z_{,\eta} ,$$

The initial displacement stiffness matrix ( due to large displacement) is given by

$$[K^{eNL}] = \int_{-1}^1 \int_{-1}^1 \left( [B^L]^T [D] [B^{NL}] + [B^{NL}]^T [D] [B^L] \right) |J| d\xi d\eta . \tag{12}$$

**Element Initial Stress Stiffness Matrix**

The non-linear strains of the shell are expressed as

$$\{\varepsilon_{xnl}, \varepsilon_{ynl}, \gamma_{xynl}\}^T = \{(w_{ox})^2/2, (w_{oy})^2/2, w_{ox} w_{oy}\}^T = [U] \{f\} / 2 , \tag{13}$$

where  $\{f\} = \{w_{,x}, w_{,y}\}^T$  and  $[U]$  is obvious from equations (13).

Using equations (9),  $\{f\}$  is expressed as

$$\{f\} = [G] \{\delta^e\} ,$$

where

$$[G] = \sum_{i=1}^8 \begin{bmatrix} 1_3 N_{i,x} & m_3 N_{i,x} & n_3 N_{i,x} & 0 & 0 \\ 1_3 N_{i,y} & m_3 N_{i,y} & n_3 N_{i,y} & 0 & 0 \end{bmatrix} ,$$

$$\{\delta^e\} = \{U_{o1}, V_{o1}, W_{o1}, \theta_{x1}, \theta_{y1}, \dots, U_{o8}, V_{o8}, W_{o8}, \theta_{x8}, \theta_{y8}\}^T .$$

The initial stress stiffness matrix of the element is given by

$$[K_{\sigma}^e] = \int_{-1}^1 \int_{-1}^1 [G]^T [S] [G] |J| d\xi d\eta , \tag{14}$$

where

$$[S] = \begin{bmatrix} N_x & N_{xy} \\ N_{xy} & N_y \end{bmatrix} .$$

The tangent stiffness matrix of the element is obtained by adding  $[K^{eL}]$ ,  $[K^{eNL}]$  and  $[K_{\sigma}^e]$ , i.e.

$$[K_T^e] = [K^{eL}] + [K^{eNL}] + [K_{\sigma}^e] . \tag{15}$$

### Element Incremental Load Vector

The incremental element load vector due to incremental uniform normal pressure  $dp_0$ , assuming that the load acts on the mid-surface of the shell, is given by

$$\{dP^e\} = \left\{ \left\{ dP^1 \right\} \dots \left\{ dP^8 \right\} \right\}^T, \quad (16)$$

$$\text{where } \{dP^i\} = \int_{-1}^1 \int_{-1}^1 N_i \{dq\} |J| d\xi d\eta,$$

$$\text{in which } \{dq\} = \{1_3 dp_0, m_3 dp_0, n_3 dp_0, 0, 0\}^T.$$

### Solution Process

Equations (11), (12), and (16) are evaluated by performing numerical integration using the 2x2 Gauss quadrature whereas equation (14) is evaluated using 3x3 Gauss quadrature. The element tangent stiffness matrices  $[K_T^e]$  and element incremental load vectors  $\{dp^e\}$  are assembled to obtain their respective global matrices  $[K_T]$  and  $\{dP\}$ . The incremental unknown displacements at the nodes of the shell are obtained from the incremental equilibrium condition

$$[K_T] \{d\delta\} = \{dP\}. \quad (17)$$

These incremental equations are solved using the Newton-Raphson iteration method [19] with the help of Gauss elimination technique [19]. Knowing the incremental displacements  $\{d\delta\}$ , the total displacements at any load level are obtained by adding the incremental displacements to displacements at the earlier load level. From the known displacements at any load level, the strains of the shell  $\{\chi\}$  are evaluated from the equations (3) and (9) and then the stress resultants are obtained from

$$\{F\} = [D] \{\chi\}, \quad (18)$$

where

$$\{\chi\} = \{\epsilon_{x0}, \epsilon_{y0}, \gamma_{xy0}, K_x, K_y, K_{xy}, \phi_x, \phi_y\}^T,$$

$$\{F\} = \{N_x, N_y, N_{xy}, M_x, M_y, M_{xy}, Q_x, Q_y\}^T.$$

### Results and Discussion

The analysis described in the previous sections is applicable for geometric non-linear analysis of various types of laminated composite shells subjected to axial and transverse load. In the present investigation, the non-linear

behaviour and the collapse pressures with the associated mode shapes are presented for symmetrically and anti-symmetrically laminated cross-ply spherical shell cap with and without a central circular cutout subjected to uniform normal pressure. The local coordinate axes  $x$  and  $y$  are always oriented along the circumferential and meridional directions, respectively. Fibre orientation angle  $\theta$  is measured with reference to circumferential direction, i.e.  $x$ -axis. Hence, fibre orientation angle  $0^\circ$  means that the fibres are along the circumferential direction, whereas fibre orientation  $90^\circ$  means that the fibres are along the meridian. It is assumed that the fibre volume in lamina is constant along the meridian. Results are presented for laminated composite spherical shell cap with and without a central circular cutout for simply supported and clamped boundary conditions. In the case of simply supported boundary condition,  $U_{0i}$  and  $V_{0i}$  are restrained along the supported edge. The following lamina material properties are used throughout the investigation.  $E_1/E_2=25$ ,  $G_{12}/E_2=0.5$ ,  $G_{13}/E_2=0.5$ ,  $G_{23}/E_2=0.2$  and  $\nu_{12}=0.25$ . For finite element analysis, the spherical shell cap without a cutout is considered as the spherical shell cap with a circular cutout with  $\phi_0 = 0.001\phi_1$ . The value of shear correction factor is assumed as  $5/6$ .

As it is difficult to get convergence of displacements while approaching the limit point, very small increments (in decimals) of pressure (load) are considered. In this way, the collapse pressure (load) is determined successfully and very accurately.

To study the convergence of collapse pressure with the increase in number of finite elements, the entire spherical shell cap is discretised with 64, 80, 96 and 112 elements. For this purpose, both symmetrically as well as anti-symmetrically laminated cross-ply spherical shell caps with simply supported and clamped boundary conditions are considered and the collapse pressures are shown in Table-1. A mesh consisting of 112 elements (Fig.1b) is employed in the present investigation. To validate the results of the present finite element analysis, two problems are considered. The first one is the geometric non-linear behaviour of isotropic clamped spherical shell cap ( $R=4.758\text{in}$ ,  $H=0.08598\text{in}$ ,  $t=0.01576\text{in}$ ,  $E=10 \times 10^6 \text{lb/in}^2$ ,  $\nu = 0.3$ ) subjected to a central concentrated load (Fig.2). In the second problem, the collapse pressure of  $[0^\circ/90^\circ/0^\circ/90^\circ/0^\circ]$  clamped spherical shell cap is compared with that available in reference [14]. From Fig.2 and Table-2, it is clear that the present finite element analysis is reliable in studying the collapse of composite spherical shell cap.

**Table-1 : Convergence of normalised collapse pressure  $p_{nc} = p_0(R/t)^4/E_2$  of laminated composite spherical shell caps ( $\phi_0 = 0.001\phi_1, \phi_1 = 10^\circ, R/t = 200$ )**

Number of elements	$[0^0/90^0/0^0/90^0/0^0]$ Simply supported	$[0^0/90^0/0^0/90^0/0^0]$ Clamped	$[0^0/90^0/0^0/90^0/0^0/90^0]$ Simply supported	$[0^0/90^0/0^0/90^0/0^0/90^0]$ Clamped
64	166944	213664	183792	293920
80	167216	213328	184352	293280
96	167216	213328	184416	293280
112	167264	213248	184448	293120

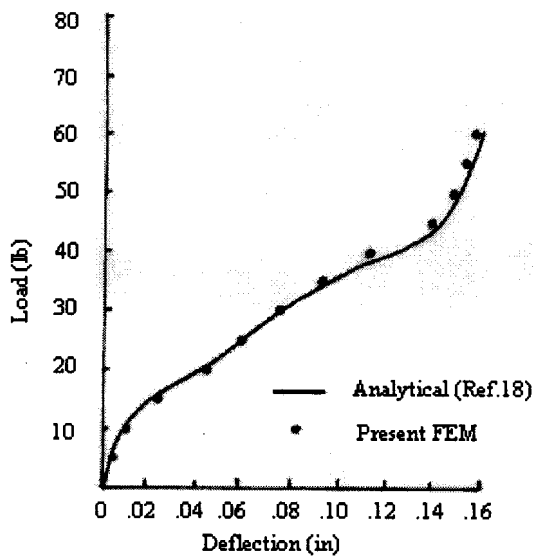


Fig. 2 Load-deflection curve for a clamped isotropic spherical shell cap under a central point load ( $\phi_0 = 0.001\phi_1, \phi_1 = 10.9035^\circ$ )

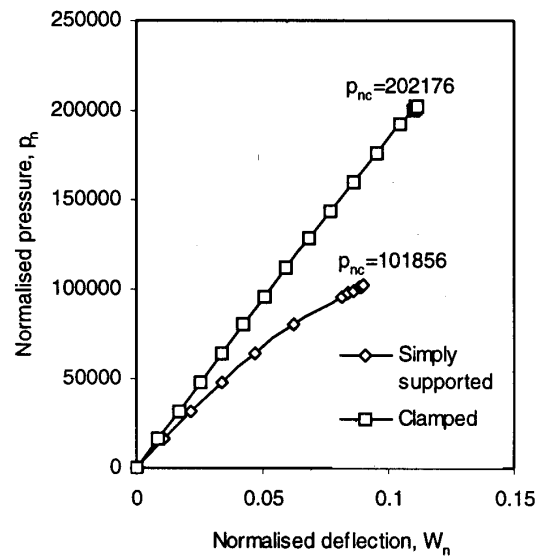


Fig. 3 Buckling response of  $[0^\circ/90^\circ]$  spherical shell cap without a cutout ( $\phi_0 = 0.001 \phi_1, \phi_1 = 10^\circ, R/t = 200$ ) under uniform normal pressure

The normalised central deflection  $W_n = W/t$  and the normalised uniform normal pressure  $p_n = p_0(R/t)^4/E_2$  are plotted for symmetrically and anti-symmetrically laminated spherical shell caps subjected to uniform normal pressure with simply supported and clamped boundary condition for  $R/t$  ratio 200. A typical plot is shown in Fig.3. The effect of number of plies ( $n$ ) on the collapse pressure is shown in Tables-3 and 4. The typical deformed shapes (mode shapes) of the spherical shell caps at the collapse pressure (i.e. at the limit point) are given in Figs. 4-5. The effect of size of the circular cutout on the collapse pressure of simply supported and clamped cross-ply laminated spherical shell caps is shown in Fig.6.

The collapse pressures are more for clamped spherical shell caps (Tables-3 and 4). The collapse pressures of simply supported symmetric and anti-symmetric spherical shell caps increase with the increase in number of layers. The collapse pressure of clamped symmetric spherical

**Table-2 : Verification of results : Collapse pressure  $p_0 a^4/E_2 t^2 H^2$  of  $[0^0/90^0/0^0/90^0/0^0]$  clamped spherical shell cap**

Present FEM	From reference [14]
10.543	10.800

shell cap also increases with the increase in number of layers but the collapse pressure of clamped anti-symmetric spherical shell cap decreases with the increase in number of layers from 4 to 12. In general, as the number of layers increases, the stiffness of the spherical cap increases and hence collapse pressure increases. But, in the case of clamped  $[0^\circ/90^\circ]$  spherical shell cap, the stiffness of the spherical shell cap is affected by the coupling between bending and extension and the restraint provided by the clamped supported edge. The deformed shapes of simply supported and clamped symmetric cross-ply laminated spherical shell caps remain spherical at the limit point as

shown in Fig.4. The deformed shapes of simply supported and clamped anti-symmetric cross-ply laminated spherical shell caps are not spherical at the limit point as shown in Fig. 5.

The collapse pressures of simply supported and clamped  $[0^\circ/90^\circ]$  spherical shell cap decrease initially (up

to  $\phi_0/\phi_1=0.1$ ) and then increases with the increase in cutout size (Fig. 6). This is due to variation in the stiffness of the spherical shell cap with the increase in cutout size. There is a greater increase in the collapse pressure of clamped  $[0^\circ/90^\circ]$  spherical shell cap beyond  $\phi_0/\phi_1=0.5$  compared to the increase in the collapse pressure of simply supported  $[0^\circ/90^\circ]$  spherical shell cap beyond  $\phi_0/\phi_1=0.5$ . This is due

**Table-3 : The effect of number of plies (n) on the normalised collapse pressure  $p_{nc} = p_o (R/t)^4/E_2$  of symmetrically laminated  $[0^\circ/90^\circ/0^\circ \dots]$  cross-ply spherical shell cap without a cutout ( $\phi_0 = 0.001\phi_1, \phi_1 = 10^\circ, R/t = 200$ )**

Boundary condition	n=3	n=5	n=7	n=9	n=11	n=13
Simply supported	148560	167264	173664	176928	178944	180320
Clamped	165360	213248	231440	240640	246352	250272

**Table-4 : The effect of number of plies (n) on the normalised collapse pressure  $p_{nc} = p_o (R/t)^4/E_2$  of anti-symmetrically laminated  $[0^\circ/90^\circ \dots]$  cross-ply spherical shell cap without a cutout ( $\phi_0 = 0.001\phi_1, \phi_1 = 10^\circ, R/t = 200$ )**

Boundary condition	n=2	n=4	n=6	n=8	n=10	n=12
Simply supported	101856	177024	184448	186592	187424	187776
Clamped	202176	294560	293120	289632	286736	284416

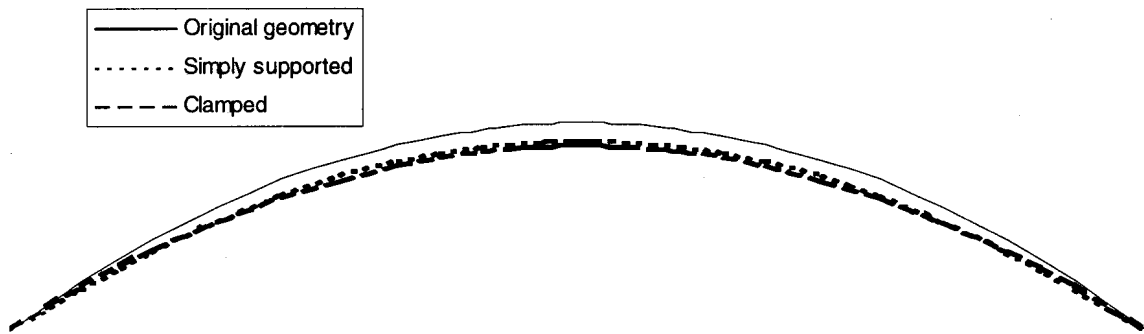


Fig. 4 Original and deformed shapes of  $[0^\circ/90^\circ/0^\circ]$  spherical shell cap without a cutout ( $\phi_0 = 0.001 \phi_1, \phi_1 = 10^\circ, R/t = 200$ ) at the limit point

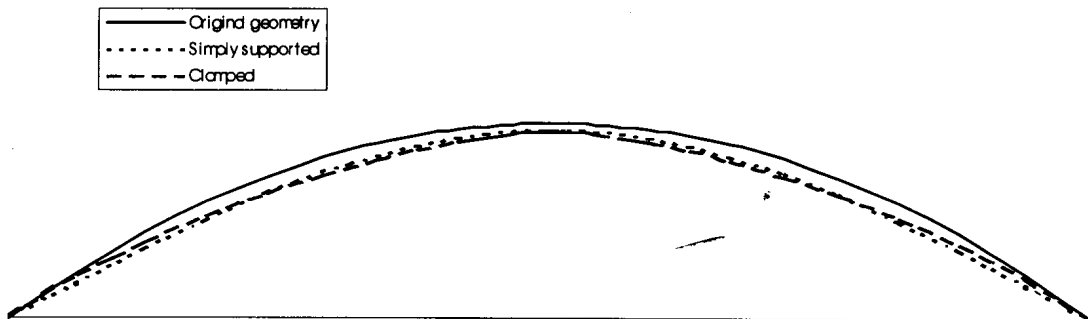


Fig. 5 Original and deformed shapes of  $[0^\circ/90^\circ]$  spherical shell cap without a cutout ( $\phi_0 = 0.001 \phi_1, \phi_1 = 10^\circ, R/t = 200$ ) at the limit point



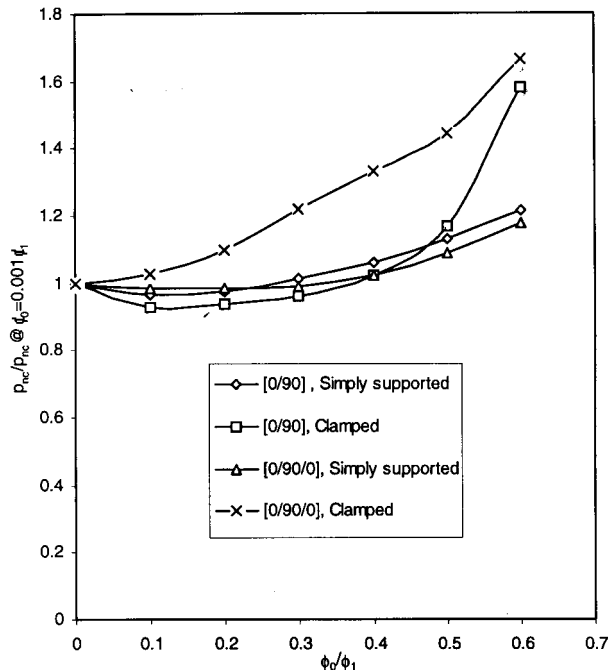


Fig. 6 Collapse pressures of laminated spherical shell caps with a central circular cutout ( $\phi_1 = 10^\circ$ )

to increased stiffness provided by the clamped supported edge. The collapse pressure of simply supported  $[0^\circ/90^\circ/0^\circ]$  laminated spherical shell cap also decreases initially (up to  $\phi_0/\phi_1=0.2$ ) and then increases with the increase in cutout size. The collapse pressure of clamped  $[0^\circ/90^\circ/0^\circ]$  spherical shell cap increases with the increase in cutout size. This is due to increase in the stiffness of the spherical shell cap with the increase in cutout size, i.e. due to stiffening effect.

### Conclusion

The buckling of laminated composite spherical shell cap with and without a cutout is investigated using a geometric non-linear finite element analysis based on the first-order shear deformation theory. The non-linear behaviour and the collapse pressures with the associated mode shapes are presented for symmetrically and anti-symmetrically laminated simply supported and clamped spherical shell caps subjected to uniform normal pressure.

The collapse pressures are more for clamped spherical shell caps with out a cutout compared to simply supported spherical shell caps with out a cutout for both symmetric and anti-symmetric laminations considered. The collapse pressures of simply supported symmetric and anti-symmetric spherical shell caps increase with the increase in

number of layers. The collapse pressures of clamped symmetric shell caps also increase with the increase in number of layers but the collapse pressures of clamped anti-symmetric spherical shell caps generally decrease with the increase in number of layers.

The collapse pressures of simply supported and clamped two layered anti-symmetrically laminated composite spherical shell caps decrease initially and then increase with the increase in cutout size. The collapse pressure of simply supported three layered symmetrically laminated spherical shell cap also decreases initially and then increases with the increase in cutout size whereas the collapse pressure of clamped three layered symmetrically laminated spherical shell cap increases with the increase in cutout size.

### References

1. Bauld, Jr, N.R. and Khot, N.S., "A Numerical and Experimental Investigation of the Buckling Behaviour of Composite Panels", Computers and Structures, Vol.15, pp.393-403,1982.
2. Jun, S.M. and Hong, C.S., "Buckling Behaviour of Laminated Composite Cylindrical Panels Under Axial Compression", Computers and Structures, Vol.29, pp.479-490,1988.
3. Palazotto, A.N. and Tisler, T.W., "Considerations of Cutouts in Composite Cylindrical Panels", Computers and Structures, Vol.29, pp.1101-1110,1988.
4. Goldmanis, M. and Riekstinsh A., "Post-buckling Finite Element Analysis of Composite Cylindrical Panels in Axial Compression", Composite Structures, Vol. 29, pp.457-462,1994.
5. Madenci, E. and Barut A., "Pre-and Post-buckling Response of Curved, Thin, Composite Panels with Cutouts Under Compression", Int. J. Num. Meth. Engg, Vol.37, pp.1499-1510,1994.
6. Simites, G.J., "Buckling of Moderately Thick Laminated Cylindrical Shells: A Review", Composites Part-B, Vol.27B, pp. 581-587,1996.
7. Kim, K.D., "Buckling Behaviour of Composite Panels Using the Finite Element Method", Composite Structures, Vol.36, pp. 33-43,1996.

8. Chaplin, C.P. and Palazotto, A.N., "The Collapse of Composite Cylindrical Panels with Various Thickness Using Finite Element Analysis", Computers and Structures; Vol.60, pp.797-815,1996.
9. Noor, A.K., Starnes Jr, J.H. and Peters, J.M., "Non-linear and Postbuckling Responses of Curved Composite Panels with Cutouts", Composite Structures, Vol.34, pp.213- 240,1996.
10. Kim, K. and Voyiadjis, G.Z., "Non-linear Finite Element Analysis of Composite Panels", Composites Part-B, Vol.30, pp. 365-381,1999.
11. Prema Kumar, W.P. and Palaninathan, R.," Non-linear Response of Laminated Cylindrical Panels", Thin Walled Structures, Vol.39, pp.519-533, 2001.
12. Hilburger, M.W., Britt, V.O. and Nameth, M.P., "Buckling Behaviour of Compression Loaded Quasi-isotropic Curved Panels with a Circular Cutout", International Journal of Solids and Structures, Vol.38, pp. 1495-1522, 2001.
13. Xu, C.S. ,"Buckling and Post-buckling of Symmetrically Laminated Moderately Thick Spherical Shells", International Journal of Solids and Structures, Vol.28, pp.1171-1184, 1991.
14. Narasimhan, M.C. and Alwar, R.S., "Axisymmetric Buckling of Antisymmetrically Laminated Spherical Caps", AIAA Journal, Vol.31, pp. 408-409, 1992 .
15. Aleksander M., "On the Buckling of Composite Shells of Revolution Under External Pressure", Composite Structures, Vol.21, pp.107-119, 1992.
16. Sai Ram, K.S. and Sreedhar Babu, T., "Buckling of Laminated Composite Shells Under Transverse Load", Composite Structures, Vol.55, pp.157-168, 2002.
17. Cook, R.D., Malkus D.S. and Plesha, M.E . "Concepts and Applications of Finite Element Analysis", Chapter 12, John Wiley, New York, 1989.
18. Zienkiewicz, O.C. and Taylor R.L., "The Finite Element Method",Chapter 5, Volume 2, McGraw-Hill, London, 1991.
19. Bathe, K.J., "Finite Element Procedures", Prentice-Hall, Englewood Cliffs, New Jersey, 1996.

## Appendix

Non zero elements of  $[B^L]$  matrix :

$$B_{1,5i-4} = 1_1 N_{i,x}, B_{1,5i-3} = m_1 N_{i,x}, B_{1,5i-2} = n_1 N_{i,x},$$

$$B_{2,5i-4} = 1_2 N_{i,y}, B_{2,5i-3} = m_2 N_{i,y}, B_{2,5i-2} = n_2 N_{i,y},$$

$$B_{3,5i-4} = 1_1 N_{i,y} + 1_2 N_{i,x}, B_{3,5i-3} = m_1 N_{i,y} + m_2 N_{i,x}, B_{3,5i-2} = n_1 N_{i,y} + n_2 N_{i,x},$$

$$B_{4,5i-1} = E_{21i} N_{i,x}, B_{4,5i} = E_{22i} N_{i,x},$$

$$B_{5,5i-1} = -E_{11i} N_{i,y}, B_{5,5i} = -E_{12i} N_{i,y},$$

$$B_{6,5i-1} = E_{21i} N_{i,y} - E_{11i} N_{i,x}, B_{6,5i} = E_{22i} N_{i,y} - E_{12i} N_{i,x},$$

$$B_{7,5i-4} = 1_3 N_{i,x}, B_{7,5i-3} = m_3 N_{i,x}, B_{7,5i-2} = n_3 N_{i,x}, B_{7,5i-1} = E_{21i} N_i, B_{7,5i} = E_{22i} N_i,$$

$$B_{8,5i-4} = 1_3 N_{i,y}, B_{8,5i-3} = m_3 N_{i,y}, B_{8,5i-2} = n_3 N_{i,y}, B_{8,5i-1} = -E_{11i} N_i, B_{8,5i} = B_{8,5i} = -E_{12i} N_i .$$

(i = 1 to 8)

Non zero elements of  $[B^{NL}]$  matrix :

$$B_{1,5i-4} = w_{0,x} l_3 N_{i,x}, B_{1,5i-3} = w_{0,x} m_3 N_{i,x}, B_{1,5i-2} = w_{0,x} n_3 N_{i,x},$$

$$B_{2,5i-4} = w_{0,y} l_3 N_{i,y}, B_{2,5i-3} = w_{0,x} m_3 N_{i,y}, B_{2,5i-2} = w_{0,y} n_3 N_{i,y},$$

$$B_{3,5i-4} = l_3 (w_{0,x} N_{i,y} + w_{0,y} N_{i,x}),$$

$$B_{3,5i-3} = m_3 (w_{0,x} N_{i,y} + w_{0,y} N_{i,x}),$$

$$B_{3,5i-2} = n_3 (w_{0,x} N_{i,y} + w_{0,y} N_{i,x}),$$

$$\text{where } w_{0,x} = l_3 \sum_{i=1}^8 N_{i,x} U_{0i} + m_3 \sum_{i=1}^8 N_{i,x} V_{0i} + n_3 \sum_{i=1}^8 N_{i,x} W_{0i},$$

$$w_{0,y} = l_3 \sum_{i=1}^8 N_{i,y} U_{0i} + m_3 \sum_{i=1}^8 N_{i,y} V_{0i} + n_3 \sum_{i=1}^8 N_{i,y} W_{0i},$$

( $i = 1, 8$ )